R. & M. No. 2120
(5950, 6126 & 6443)
A.R.C. Technical Report

MINISTRY OF SUPPLY

AERONAUTICAL RESEARCH COUNCIL
REPORTS AND MEMORANDA

The Smallest Size of a Spanwise Surface Corrugation which affects Boundary-layer Transition on an Aerofoil

By

A. FAGE, F.R.S.,
of the Aerodynamics Division, N.P.L.

LONDON: HIS MAJESTY'S STATIONERY OFFICE
Price 3*s.* 6*d.* net

The Smallest Size of a Spanwise Surface Corrugation which affects Boundary-layer Transition on an Aerofoil

By

A. FAGE, F.R.S.,
of the Aerodynamics Division, N.P.L.

Reports and Memoranda No. 2120

January, 1943*

Summary.—The effect of a spanwise surface corrugation on the position of transition from laminar to turbulent flow in the boundary layer of an aerofoil depends on the local disturbances caused by the corrugation and on the stability of flow in the laminar boundary layer beyond. The report describes wind-tunnel experiments made for bulges, hollows and ridges on an aerofoil and on a flat plate to obtain relations for the minimum height of a spanwise surface corrugation which affects the position of boundary-layer transition, and so the drag, of a laminar-flow aerofoil.

Two empirical relations are obtained

$$\text{(i)}\ \frac{h}{L} = 13{\cdot}5 \times 10^6 \left[\frac{u_{1c}L}{\nu}\right]^{-3/2} \left[\frac{X}{L}\right]^{1/2} \left[\frac{B}{L}\right]^{1/2} \text{for the condition } \left(\frac{B}{L}\right)^{1/2}\left(\frac{X}{L}\right)^{1/2} < 0{\cdot}09$$

and

$$\text{(ii)}\ \frac{h}{L} = 9{\cdot}0 \times 10^6 \left[\frac{u_{1c}L}{\nu}\right]^{-3/2} \left[\frac{B}{L}\right]^{1/2} \text{for the condition } \left(\frac{B}{L}\right)^{1/2}\left(\frac{X}{L}\right)^{1/2} > 0{\cdot}09,$$

where h is the minimum height, L is the length of the laminar boundary layer, u_{1c} is the velocity just outside the layer at the corrugation position, B is the width of the corrugation and X is the distance of the corrugation behind the leading edge of the aerofoil. The range of $u_{1c}L/\nu$ covered is 10^6 to $3{\cdot}5 \times 10^6$.

The experiments show that the minimum height is not especially dependent on the form of the corrugation, and that the rising and falling velocity gradients associated with a corrugation which just affects transition are numerically large compared with the beneficial rising velocity gradient on a smooth laminar-flow aerofoil.

The flow on and near a corrugation is examined from measurements of normal pressure on the surface. It appears that the flow conditions near a corrugation which affects transition position are associated with a separation of the laminar boundary layer from its surface.

1. *Introduction.*—The effect of a spanwise surface corrugation on the position of transition from laminar to turbulent flow in the boundary layer of an aerofoil depends on the local disturbances caused by the corrugation and on the stability of flow in the laminar boundary layer beyond. The report describes wind-tunnel experiments made for bulge, hollow and ridge corrugations on an aerofoil and on a flat plate to obtain data needed to allow empirical relations to be derived which would give a rough estimate for the minimum height of a spanwise surface corrugation which affects the position of boundary-layer transition, and so the drag, of a laminar-flow aerofoil. The conditions under which the experiments were made were such that the results obtained are not likely to be affected by turbulence in the wind-tunnel stream nor by surface roughness due to small excresences. The effect of velocity gradient in the direction of flow along the surface is considered. The conditions of flow on and near smooth bulge and hollow

* This report comprises A.R.C. 5950 (July, 1942), 6126 (September, 1942) and 6443 (January, 1943).

corrugations are deduced from surface pressure measurements. The experiments on the flat plate were made by W. S. Walker and J. R. Greening and those on the aerofoil by W. S. Walker and R. J. Cox. Results obtained by Dr. G. S. Hislop from experiments made at Cambridge for narrow spanswise surface ridge corrugations on a flat plate are included for analysis.

2. *Notation*

x	distance from leading edge, measured along plate or aerofoil chord
X	distance of centre line of bulge, ridge, hollow from leading edge
x_1	distance from centre line of bulge, ridge, hollow
y	normal distance from surface
y_1	shape ordinate
h	height of bulge, ridge, depth of hollow
h_e	effective distance from the surface to which the velocity given by a surface tube is related
B	width of bulge, ridge, hollow
c	aerofoil chord
L	length of laminar boundary layer
U_0	datum free stream velocity
u	velocity in boundary layer
u_1	velocity just outside boundary layer
u_{1c}	velocity just outside boundary layer at the position of the centre line of a corrugation but for the undistorted surface
u_h	velocity at normal distance h from surface of uncorrugated plate or aerofoil
Δu_1	change in u_1 due to bulge, ridge, hollow
p_0	datum free stream pressure
p	normal pressure on surface
Δp	change in p due to bulge, ridge and hollow
ϑ	momentum thickness of boundary layer
δ	thickness of boundary layer

$$\Lambda = \frac{\delta^2}{\nu}\frac{du_1}{dx}.$$

3. *Corrugations on a Flat Plate.*—3.1. These experiments were made in the 13 ft. × 9 ft. tunnel for smooth bulges, flat ridges and smooth hollows on one side of a smooth flat aluminium plate, 6 ft. × 3 ft. × 0·5 in., having an elliptical leading edge. The plate, with plywood extension sheets, 6 ft. × 3 ft. × 0·5 in., was mounted vertically between the floor and roof of the tunnel, with the 6-ft. length downstream and the experimental surface about 4 ft. from a wall. A rising velocity in the direction of flow was obtained by an inclination of the plate to the near wall. For one of the streams (B) a fairing was fitted to the tunnel wall to modify the velocity gradient near the leading edge of the plate. The flow in the 13 ft. × 9 ft. tunnel is sufficiently steady to allow the properties of low-drag aerofoils to be investigated at wind speeds below 140 f.p.s. The experiments were made for bulges, ridges and hollows whose height (or depth) were such that they affected transition position at speeds well below 140 f.p.s., to ensure that transition was

not affected by turbulence in the wind-tunnel stream. Measurements were made for two wind-tunnel streams, designated A and B respectively. For stream A the values of A, $(du_1/dx)_{x=X}$ and $(du_1/dx)_{x>1\cdot3X}$ (*see* § 2 Notation) for the plate without a corrugation were $1\cdot35$, $0\cdot032\ U_0$ and $0\cdot018\ U_0$ respectively. For stream B, the values were $0\cdot90$, $0\cdot018\ U_0$ and $0\cdot008\ U_0$ respectively. The datum velocity U_0 was measured in the undisturbed stream at the station $x = X$.

3.2. The smooth bulges and hollows were formed by bulging a strip of spring steel, $0\cdot02$-in. thick, 4-in. wide and 32-in. span, recessed into the aluminium plate. The centre line of the strip was 20 in. behind the leading edge of the plate. The method of forming a bulge or hollow is illustrated in Fig. 1. Small circular discs, *a*, soldered on the undersurface of the strip near its leading and trailing edges, were located in circular recesses in the aluminium plate. The depths of the recesses were carefully adjusted so that the upper surface of the strip near the leading and trailing edges was flush with the surface of the aluminium plate when the discs were pulled hard down into their recesses by the fine-thread pins, *c*. The strip was bulged by a thin steel bar *b* forced upwards by pins screwed into the plate below. The height of a bulge was adjusted by first loosening the clamping pins at the trailing edge, pushing the bar upwards, and finally screwing the trailing-edge discs hard down. The recesses at the trailing edge had a slightly larger diameter than that of the discs to permit small lateral displacement due to strip distortion. Smooth hollows were formed in the same manner as that for the bulges, except that the strip was pulled down along its centre line, the aluminium plate under the strip being suitably hollowed out. The shape taken by the strip was measured with an Ames dial, reading to $0\cdot0005$ in., traversed along a bar carried on two legs resting on the aluminium plate. The theoretical shape is that taken by a 4-in. strip rigidly clamped along its longer edges and loaded uniformly along its centre line, Appendix (*a*). Figs. 2 and 15 show that the measured ordinates of the bulges and hollows agree with the theoretical values within $\pm\ 0\cdot05h$. Actually, the maximum ordinates were not at the middle of the strip, but were displaced about $0\cdot1$ to $0\cdot2$ in. towards the leading edge.

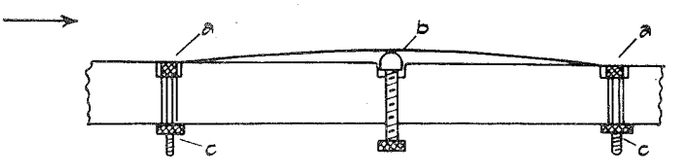

FIG. 1

3.3. Small surface tubes mounted on the plate were used to indicate when a corrugation caused transition in the laminar layer beyond to move forward. The scheme of experiment was to increase, for corrugations of known height (or depth), the wind speed, U_0 until the reading of a surface tube, r, indicated that a change from laminar to turbulent flow had occurred at the position occupied by the tube. It is shown in Appendix (*d*) that the change occurs when the value of $(1/K)\ (r/U_0^3)^{1/2}$, where K is the value of $(r/U_0^3)^{1/2}$ for laminar flow, departs from unity. Representative curves of $(1/K)\ (r/U_0^3)^{1/2}$ are plotted against U_0X/ν in Fig. 5, where X is the distance of the centre line of a corrugation behind the leading edge of the plate. It is seen that the rise in $(1/K)\ (r/U_0^3)^{1/2}$ is quite steep for an increase in U_0X/ν beyond the value for which transition occurs.

Surface tubes were mounted $2\cdot08$, $2\cdot92$, $3\cdot75$ and $4\cdot57$ ft. behind the leading edge of the plate. The tubes at $2\cdot08$ and $3\cdot75$ ft. were offset 3 in. on one side of the centre line of the plate, and those at $2\cdot92$ and $4\cdot57$ ft. the same distance on the other side. The tubes at $2\cdot08$ and $2\cdot92$ ft. were removed before taking readings with the tubes at $3\cdot75$ and $4\cdot57$ ft. A diagrammatic sketch of the shape of a tube is given in Fig. 4. The tube openings were about $0\cdot002$ in.

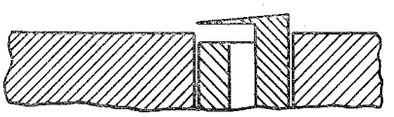
FIG. 4.—Surface Tube.

The experimental results obtained for the corrugations are collected in Table 1. They are analysed later in Section 6.

TABLE 1

Experiments on Flat Plate. $X = 1{\cdot}667$ *ft.* *Transition at* $x = L$

$\left(\frac{u_{1c}L}{\nu}\right)$ range covered, $1{\cdot}2 \times 10^6$ to $2{\cdot}4 \times 10^6$

	u_{1c} ft./sec.	h in.	L ft.	$\left(\frac{B}{L}\right)^{1/2}\left(\frac{X}{L}\right)^{1/2}$	$\frac{h}{L}\left(\frac{u_{1c}L}{\nu}\right)^{3/2}\left(\frac{X}{L}\right)^{1/2}10^{-6}$	$\frac{h}{L}\left(\frac{u_{1c}L}{\nu}\right)^{3/2}10^{-6}$
Smooth bulge	82·6	0·0310	4·58	0·163	1·25	2·07
$A_X = 0{\cdot}90$	69·4	0·0525	4·58	0·163	1·50 } 1·34	2·49 } 2·23
	53·0	0·0620	4·58	0·163	1·28	2·12
$B = 4$ in.	78·0	0·0530	3·75	0·199	1·96 } 1·79	2·94 } 2·68
	61·5	0·0620	3·75	0·199	1·61	2·42
Stream B	95·0	0·0525	2·92	0·256	2·60 } 2·29	3·44 } 3·02
	70·0	0·0620	2·92	0·256	1·97	2·61
	92·4	0·0620	2·08	0·358	2·94	3·29
Smooth bulge	70·4	0·0555	4·58	0·163	1·77	2·93
$A_X = 1{\cdot}35$	56·2	0·0665	4·58	0·163	1·48 } 1·58	2·46 } 2·62
	53·8	0·0700	4·58	0·163	1·49	2·48
$B = 4$ in.	76·0	0·0555	3·75	0·199	1·97	2·95
	62·4	0·0630	3·75	0·199	1·67 } 1·71	2·51 } 2·57
Stream A	55·5	0·0680	3·75	0·199	1·50	2·25
Flat ridge	60·1	0·0245	4·58	0·077	0·61 } 0·54	1·01 } 0·89
$A_X = 0{\cdot}90$	58·3	0·0195	4·58	0·077	0·46	0·76
	70·3	0·0245	3·75	0·094	0·78 } 0·80	1·17 } 1·20
$B = 0{\cdot}9$ in.	84·9	0·0195	3·75	0·094	0·82	1·23
	89·3	0·0245	2·92	0·121	1·12 } 1·04	1·48 } 1·38
Stream B	94·2	0·0195	2·92	0·121	0·96	1·27
Smooth hollow	65·8	0·067	4·58	0·163	1·92 } 1·98	3·18 } 3·28
$A_X = 1{\cdot}35$	76·4	0·057	4·58	0·163	2·04	3·38
	61·9	0·067	3·75	0·199	1·76 } 2·03	2·64 } 3·04
$B = 4$ in.	82·7	0·057	3·75	0·199	2·29	3·44
	69·7	0·067	2·92	0·256	2·09 } 2·24	2·77 } 2·97
Stream A	84·9	0·057	2·92	0·256	2·39	3·16

4. *Corrugations on Aerofoil* EQH 1260.—4.1. These experiments were made for three forms of narrow spanwise corrugations, flat, arch and wire, situated in the laminar boundary layer of a large symmetrical aerofoil, EQH 1260 section, mounted at 0 deg. incidence between the floor and roof of the 13 ft. × 9 ft. tunnel. The chord of the aerofoil was 70·4 in. The scheme of experiment was to measure, for corrugations of known height, the wind speed, U_0, for which the drag of the aerofoil, measured by the pitot-traverse method, began to rise, owing to a forward movement of transition caused by a corrugation. The aerofoil was made of wood and covered with a thin metal sheet to obtain a smooth skin. The curve of C_{D_0} against U_0c/ν for the aerofoil without a corrugation is given in Figs. 6 and 7. With an increase in U_0c/ν, C_{D_0} falls continuously to a minimum value, about 0·0029, at $U_0c/\nu = 6 \times 10^6$, and then rises rapidly. This rise is caused by a forward movement of transition due mainly to wind-tunnel turbulence. Transition occurs at about $0{\cdot}8c$ for $U_0c/\nu < 6 \times 10^6$.

4.2. The flat and arch ridges were 1 in. wide and they were formed by strips of Lassoelastic adhesive tape, about 0·002-in. thick. The strips forming an arch ridge increased in width, with the distance from the surface, from 0·25 in. to 1 in. An arch ridge had, therefore, a corrugated surface, the number of the corrugations increasing with the number of strips and so with

the height of the ridge. The wire ridges were formed by piano wire. The ridges were placed in the laminar boundary layer at the stations $X = 0{\cdot}067c$, $0{\cdot}24c$ and $0{\cdot}40c$. Over this part of the aerofoil the velocity, u_1 just outside the layer rises gradually in the direction of flow (Fig. 8). The values of $(c/U_0)\,(du_1/ds)$, where s is the distance along the surface, at these stations are $0{\cdot}34$, $0{\cdot}05$ and $0{\cdot}05$ respectively. The height of a ridge above the aerofoil surface was measured with a curvature gauge.

4.3. Curves of C_{D_0} (uncorrected for tunnel-wall constraint) for the aerofoil without and with the single corrugations, plotted against the Reynolds number, U_0c/ν, of the aerofoil are given in Figs. 6 and 7. The value of U_0c/ν for which a corrugation just causes the drag of the aerofoil to rise is well defined in all cases. Also these values of U_0c/ν are well below the value, 6×10^6, at which turbulence in the wind-tunnel stream causes a rise in the value of C_{D_0} for the aerofoil alone. The experimental results obtained for the corrugations are collected in Table 2. They are analysed later in Section 6.

TABLE 2

Experiments on Aerofoil EQH 1260

$B = 1$ in. $\quad L = 4{\cdot}69$ ft. $\quad A_X \simeq 0{\cdot}45$. $\quad$ Transition at $x = L$

$\frac{u_{1c}L}{\nu}$ range covered, 2×10^6 to $3{\cdot}5 \times 10^6$

	u_{1c} ft. sec.	X ft.	h in.	$\left(\frac{B}{L}\right)^{1/2}\left(\frac{X}{L}\right)^{1/2}$	$\frac{h}{L}\left(\frac{u_{1c}L}{\nu}\right)^{3/2}\left(\frac{X}{L}\right)^{1/2} 10^{-6}$	$\frac{h}{L}\left(\frac{u_{1c}L}{\nu}\right)^{3/2} 10^{-6}$
Flat ridge ..	67·4	0·39	0·0140	0·038	0·200	0·693
	84·2	0·39	0·0067	0·038	0·158 } 0·17	0·548 } 0·58
	114	0·39	0·0047	0·038	0·148	0·514
Flat ridge ..	75·6	1·41	0·0190	0·073	0·614	1·120
	71·2	1·41	0·0180	0·073	0·530 } 0·55	0·967 } 1·01
	89·2	1·41	0·0123	0·073	0·510	0·931
	109	1·41	0·0100	0·073	0·560	1·023
Flat ridge ..	119	2·34	0·0125	0·094	1·029 } 0·98	1·456 } 1·39
	102	2·34	0·0142	0·094	0·933	1·320
Arch ridge ..	83	1·41	0·0174	0·073	0·648	1·182
	120	1·41	0·0087	0·073	0·558 } 0·54	1·018 } 0·99
	115	1·41	0·0069	0·073	0·419	0·764

4.4. Fig. 9 gives the effect on C_{D_0} of more than one surface corrugation. The curves of C_{D_0} against U_0c/ν given are for two $0{\cdot}174$-in. arch ridges, the front ridge being situated at $X = 0{\cdot}24c$ and the back ridge at $X = 0{\cdot}55c$, for two $0{\cdot}0123$-in. flat ridges at $X = 0{\cdot}24c$ and $0{\cdot}40c$ respectively, and four $0{\cdot}0069$-in. arch ridges at $X = 0{\cdot}24c$, $0{\cdot}34c$, $0{\cdot}44c$ and $0{\cdot}54c$ respectively. Curves for single ridges situated at the position of the first ridge of each set are also given. The value of U_0c/ν for which C_{D_0} begins to rise is not much less for each set than that for the front ridge alone. It appears, therefore, that it is the disturbance at the first ridge which matters most. This result is not surprising since the ridges of each set are widely spaced and the value of U_0c/ν at which C_{D_0} begins to rise for a ridge of given height increases with X.

4.5. Figs. 6 and 7 give curves of C_{D_0} against U_0c/ν for two fixed positions of transition, $x = 0{\cdot}24c$ and $x = 0{\cdot}40c$ respectively. Fig. 6 shows that the $0{\cdot}0190$-in. wire ridge brings transition to the station $X = 0{\cdot}24c$ where it is situated when $U_0c/\nu = 3{\cdot}4 \times 10^6$. The corresponding value of u_hh/ν, where u_h is the velocity in the boundary layer (without wire) at a distance

h from the surface, is 385. This value is in close agreement with the values given in Ref. 1, obtained from measurements made for wires on a long streamline body of revolution in a water tunnel.

4.6. The 0·0180-in. flat ridge brings transition to the station $X = 0{\cdot}24c$ where it is situated when $U_0c/\nu = 5{\cdot}7 \times 10^6$ (Fig. 6), and the 0·0174-in. arch ridge at $X = 0{\cdot}24c$ when $U_0c/\nu = 6{\cdot}4 \times 10^6$ (Fig. 7). The corresponding values of u_kh/ν are 730 and 810. The values of u_kh/ν for the two ridges when they just cause C_{D_0} to rise are 204 and 240 respectively. The value of u_kh/ν when transition is just brought to each ridge is therefore about four times the value when it just causes transition to move forward.

5. *Corrugations on a Flat Plate, Cambridge Experiments.*—5.1. Measurements of the effect of flat surface ridges on transition in the boundary layer of a flat glass plate have been made by Dr. G. S. Hislop at the Engineering Laboratory, Cambridge. These experiments are closely related to those described above in Section 3. For this reason they are included, with Dr. Hislop's kind permission, in the present report.

5.2. Dr. Hislop's experiments were made for three lengths of laminar boundary layer. The flat ridges were formed by layers of thin adhesive tape. A 0·00025-in. diameter hot wire was used, in conjunction with an amplifier and cathode ray oscillograph, to detect changes in the character of the flow in the boundary layer. The position of the transition point for the plate without a ridge, and so the length, L_p, of the laminar layer, was determined by a surface pitot tube. Hot wire records taken a short distance, l, forward of the pitot-tube transition point showed the flow to be always laminar but at the pitot-tube transition point the layer appeared to be laminar for about 50 per cent. of the time of observation. The method of experiment was to move a ridge progressively forward and to record the greatest distance, X, from the leading edge of the plate for which the hot wire recorded a 100 per cent. turbulent layer. The corresponding transition position which would be measured by a surface pitot tube would then be approximately a distance l forward of the position occupied by the hot wire. The length, L, of the laminar boundary layer that would be obtained from a surface tube observation of transition is then $(L_p - 2l)$ approximately. The method gives therefore a rough measure of the position of a ridge when it is just about to cause a forward movement of the transition point, provided that the value of $l/(L_p - X)$ is small. Dr. Hislop's observations were made for 17 ridge positions covering a range of $l/(L - X)$ from 0·03 to 0·53. The results selected for inclusion here are those for which $l/(L - X) < 0{\cdot}11$ and $0{\cdot}006 < h < 0{\cdot}022$. These results are given in Table 3. They are analysed in Section 6.

TABLE 3

Cambridge Experiments on a Flat Plate

Flat ridges. $B = 0{\cdot}5$ in. $\Lambda_X = 0$. Transition at $x = L$

$\left(\frac{u_{1c}L}{\nu}\right)$ range covered, $1{\cdot}7 \times 10^6$ to $2{\cdot}3 \times 10^6$

u_{1c} ft./sec.	L_p ft.	$L = (L_p - 2l)$ ft.	X ft.	h in.	$\left(\frac{B}{L}\right)^{1/2}\left(\frac{X}{L}\right)^{1/2}$	$\frac{h}{L}\left(\frac{u_{1c}L}{\nu}\right)^{3/2}\left(\frac{X}{L}\right)^{1/2} 10^{-6}$	$\frac{h}{L}\left(\frac{u_{1c}L}{\nu}\right)^{3/2} 10^{-6}$
110	3·67	3·47	2·38	0·022	0·091	1·440	1·74
110	3·67	3·47	1·94	0·012	0·082 } 0·086	0·712 } 0·83	0·95 } 1·09
102	2·67	2·27	0·79	0·0089	0·085	0·337	0·58
102	2·67	2·27	0·83	0·0106	0·080 } 0·070	0·412 } 0·45	0·68 } 0·78
110	3·67	3·47	1·07	0·011	0·060	0·486	0·88
112	1·92	1·58	0·23	0·0078	0·060 } 0·051	0·183 } 0·19	0·48 } 0·48
110	3·67	3·49	0·54	0·006	0·042	0·188	0·48

6. *Analysis of Experimental Results.*—6.1. An inspection of the results obtained from the flat-plate and aerofoil experiments, given in Tables 1, 2 and 3, shows that the minimum height, h, of a surface corrugation which affects the position of transition depends on the width, B, of the corrugation, the distance, X, of the corrugation from the leading edge of the plate or aerofoil, the length, L, of the laminar boundary layer and the velocity, u_{1c}, just outside the boundary layer at the corrugation position (but for the undistorted surface), and also that corrugation shape and velocity gradient along the plate are, for the experiments made, relatively unimportant parameters. The ration h/L can therefore be taken, as a first approximation, to be a function of X/L, B/L and $(u_{1c}L/\nu)$ only, so that we can write

$$\frac{h}{L} = \mathrm{K}\left[\frac{u_{1c}L}{\nu}\right]^{a}\left(\frac{B}{L}\right)^{b}\left(\frac{X}{L}\right)^{c},$$

where K, a, b and c are constants. Further, it was apparent from the results that a satisfactory value for b is $0{\cdot}5$. The analysis therefore resolves itself into finding the values of the constants K, a and c which would allow the relation to represent adequately the experimental results.

6.2. Calculated values of $(h/L)\,(u_{1c}L/\nu)^{3/2}$, $(h/L)\,(u_{1c}L/\nu)^{3/2}\,(X/L)^{1/2}$ and $(B/L)^{1/2}\,(X/L)^{1/2}$ are given in Tables 1, 2 and 3. Tables 1 and 2 also give average values of $(h/L)\,(u_{1c}L/\nu)^{3/2}$ and of $(h/L)\,(u_{1c}L/\nu)^{3/2}\,(X/L)^{1/2}$ for those cases for which more than one value was obtained for the same value of $(B/L)^{1/2}\,(X/L)^{1/2}$, and Table 3 average values of these quantities for group-average values of $(B/L)^{1/2}\,(X/L)^{1/2}$. The average values of $(h/L)\,(u_{1c}L/\nu)^{3/2}\,(X/L)^{1/2}$ given in Tables 1, 2 and 3 are plotted against $(B/L)^{1/2}\,(X/L)^{1/2}$ in Fig. 10. It is seen that the values for $(B/L)^{1/2}\,(X/L)^{1/2} > 0{\cdot}09$ lie reasonably closely to a straight line given by the relation

$$\frac{h}{L} = 9 \times 10^{6}\left(\frac{u_{1c}L}{\nu}\right)^{-3/2}\left(\frac{B}{L}\right)^{1/2},$$

and that the values for $(B/L)^{1/2}\,(X/L)^{1/2} < 0{\cdot}09$ lie below this line. Average values of $(h/L)\,(u_{1c}L/\nu)^{3/2}$ for the condition $(B/L)^{1/2}\,(X/L)^{1/2} < 0{\cdot}09$ are plotted against $(B/L)^{1/2}\,(X/L)^{1/2}$ in Fig. 11. It is seen that the values obtained from the N.P.L. experiments can be represented by the relation

$$\frac{h}{L} = 13{\cdot}5 \times 10^{6}\left(\frac{u_{1c}L}{\nu}\right)^{-3/2}\left(\frac{B}{L}\right)^{1/2}\left(\frac{X}{L}\right)^{1/2},$$

whilst those from the Cambridge experiments give

$$\frac{h}{L} = 11{\cdot}0 \times 10^{6}\left(\frac{u_{1c}L}{\nu}\right)^{-3/2}\left(\frac{B}{L}\right)^{1/2}\left(\frac{X}{L}\right)^{1/2}.$$

The conclusions to be drawn from the N.P.L. experiments are, therefore, that the minimum height, h, of a spanwise surface corrugation that affects transition is given by

$$\frac{h}{L} = 9 \times 10^{6}\left(\frac{u_{1c}L}{\nu}\right)^{-3/2}\left(\frac{B}{L}\right)^{1/2}, \qquad \ldots\ \ldots\ \ldots\ \ldots\ \ldots\ \ldots \quad (1)$$

when $(B/L)^{1/2}\,(X/L)^{1/2} > 0{\cdot}09$, and by

$$\frac{h}{L} = 13{\cdot}5 \times 10^{6}\left(\frac{u_{1c}L}{\nu}\right)^{-3/2}\left(\frac{B}{L}\right)^{1/2}\left(\frac{X}{L}\right)^{1/2}, \qquad \ldots\ \ldots\ \ldots\ \ldots\ \ldots \quad (2)$$

when $(B/L)^{1/2}\,(X/L)^{1/2} < 0{\cdot}09$.

It should be noted that relation (1) was obtained mainly from experiments made for smooth bulges and hollows some distance beyond the leading edge of a flat plate and that relation (2) was obtained mainly from flat and arch ridges on an aerofoil and on a flat plate closer to the leading edge. It is apparent that the two relations will not give the same value of h for the condition

$$\left(\frac{B}{L}\right)^{1/2}\left(\frac{X}{L}\right)^{1/2} = 0{\cdot}09,$$

except for the particular case $X = 0{\cdot}445L$ and $B = 0{\cdot}0182L$. Actually, the value given by relation (2) is $1{\cdot}5\ (X/L)^{1/2}$ times that given by relation (1). The lowest values of X/L in the N.P.L. experiments was about $0{\cdot}083$ (aerofoil), and the value of h given by relation (2) is then $0{\cdot}43$ the value given by relation (1).

6.3. Table 4 gives estimates of h obtained from the above relations for corrugations of width $0{\cdot}5$, 1, 3 and 6 in. on the wing of an aeroplane flying at 200, 300 and 400 m.p.h. at 20,000 ft. The length of the laminar boundary layer is taken to be $0{\cdot}7c$ and the wing chord, c, to be 10 ft. The estimates are obtained on the assumption that the relations hold for values of $u_{1c}L/\nu$ appreciably greater than those covered in the wind-tunnel experiments from which the relations were obtained. The estimates are included to give a rough practical measure of the height of a corrugation which affects transition and so the wing drag.

TABLE 4

Corrugation height, h, in inches. *Wing chord* = 10 *ft.* $L = 7$ *ft.*

B in.	$\frac{X}{L}$	$\left(\frac{B}{L}\right)^{1/2}\left(\frac{X}{L}\right)^{1/2}$	Aeroplane Speed, m.p.h.		
			200	300	400
$0{\cdot}5$	$0{\cdot}1$	$0{\cdot}024$	$0{\cdot}001$	$0{\cdot}0006$	$0{\cdot}0004$
	$0{\cdot}4$	$0{\cdot}049$	$0{\cdot}002$	$0{\cdot}001$	$0{\cdot}0008$
	$0\ 7$	$0{\cdot}064$	$0{\cdot}002$	$0{\cdot}001$	$0{\cdot}0008$
1	$0{\cdot}1$	$0{\cdot}034$	$0{\cdot}0015$	$0{\cdot}001$	$0{\cdot}0005$
	$0{\cdot}4$	$0{\cdot}069$	$0{\cdot}003$	$0{\cdot}0015$	$0{\cdot}001$
	$0{\cdot}7$	$0{\cdot}091$	$0{\cdot}003$	$0{\cdot}0015$	$0{\cdot}001$
3	$0{\cdot}1$	$0{\cdot}060$	$0{\cdot}003$	$0{\cdot}0015$	$0{\cdot}001$
	$0{\cdot}4$	$0{\cdot}120$	$0{\cdot}005$	$0{\cdot}003$	$0{\cdot}002$
	$0{\cdot}7$	$0{\cdot}158$	$0{\cdot}005$	$0{\cdot}003$	$0{\cdot}002$
6	$0{\cdot}1$	$0{\cdot}084$	$0{\cdot}004$	$0{\cdot}002$	$0{\cdot}001$
	$0{\cdot}4$	$0{\cdot}169$	$0{\cdot}007$	$0{\cdot}004$	$0{\cdot}003$
	$0{\cdot}7$	$0{\cdot}224$	$0{\cdot}007$	$0{\cdot}004$	$0{\cdot}003$

6.4. The results given in § 4.6 show that a flat ridge, $h = 0{\cdot}0180$ in., $B = 1{\cdot}0$ in., situated on the aerofoil EQH 1260 at $X = 0{\cdot}24c = 16{\cdot}9$ in. brings transition to the station where it is situated when $U_0c/\nu = 5{\cdot}7 \times 10^6$ and the $0{\cdot}0174$ in. arch ridge, $B = 1{\cdot}0$ in., situated at the same station when $U_0c/\nu = 6{\cdot}4 \times 10^6$. For these conditions $(B/L)^{1/2}\,(X/L)^{1/2} = 0{\cdot}243$ and the values of $u_{1c}L/\nu$ are $1{\cdot}525 \times 10^6$ and $1{\cdot}715 \times 10^6$ respectively. The values of h calculated from the relation

$$\frac{h}{L} = 9 \times 10^6 \left(\frac{u_{1c}L}{\nu}\right)^{-3/2}\left(\frac{B}{L}\right)^{1/2}$$

are $0{\cdot}0195$ in. for the flat ridge and $0{\cdot}0164$ in. for the arch ridge. These calculated values are within $\pm$ 8 per cent. of the actual heights.

7. *Flight Experiments.*—Estimations of the minimum height, h, of a corrugation which affects transition from the above relations 1 and 2 if made for values of $u_{1c}L/\nu$ appreciably greater than the values covered in the wind-tunnel experiments must be accepted with caution. It is, however, possible to obtain an idea of the accuracy of estimation for values of $u_{1c}L/\nu$ higher than the wind-tunnel values from a comparison with results obtained from measurements, made at the Royal Aircraft Establishment, for flat ridges, arch ridges and smooth bulges on aeroplane

wings in flight (Refs. 2 and 3). The flat ridges were formed by strips of adhesive tape and the arch ridges by strips of tape of different width. The smooth bulges were formed by several coatings of paint, rubbed down to give a smooth surface. The flight values of $u_{1c}L/\nu$ range from $1{\cdot}8 \times 10^6$ to $5{\cdot}1 \times 10^6$. The results obtained are given in Table 5. The last but one column gives the height, h, calculated from relation 1 for $(B/L)^{1/2}\ (X/L)^{1/2} > 0{\cdot}09$. The last column gives the ratios of the calculated height to the actual height. It is seen that these ratios range from 0·6 to 2·0. The average of the ratios in the last column gives 1·3, so that the calculated height is 30 per cent. greater than the actual height. This difference is not unsatisfactory in view of the character of the problem.

TABLE 5

	Flight Data							Calculated height h in.	Calculated height / Actual height
	C_L	B in.	X ft.	L ft.	$\left(\frac{u_{1c}L}{\nu}\right)10^{-6}$	$\left(\frac{B}{L}\right)^{1/2}\left(\frac{X}{L}\right)^{1/2}$	Height h in.		
Flat and arch ridges on the lower surface of wing section E Q B 19.7.50/12.5.58 on "Falcon" aeroplane[2].	0·21	0·5	0·867	1·91	2·98	0·099	0·003	0·0059	2·0
	0·26	0·5	0·867	2·33	3·17	0·082	0·003	0·0060	2·0
	0·21	0·5	1·85	2·93	4·63	0·095	0·003	0·0038	1·3
	0·26	0·5	1·85	3·28	4·58	0·084	0·003	0·0041	1·4
	0·21	1·0	1·85	2·81	4·43	0·140	0·006	0·0056	0·9
	0·26	1·0	1·85	2·87	4·00	0·137	0·006	0·0067	1·1
	0·21	1·5	1·85	2·51	3·97	0·192	0·009	0·0076	0·8
	0·21	1·5	0·867	1·315	2·05	0·251	0·009	0·0149	1·7
	0·26	1·5	0·867	1·315	1·79	0·251	0·009	0·0184	2·0
Smooth bulges on upper surface of wing section NACA 15,47/18,47 on "Falcon" aeroplane[3].	0·35	2·75	2·0	2·71	3·82	0·251	0·020	0·0114	0·6
	0·35	5·5	2·0	3·59	5·07	0·268	0·020	0·0120	0·6

8. *Flow on and near a Corrugation.*—8.1. Normal pressures on and near five bulges were measured for $U_0 = 62{\cdot}3$ and 120 f.p.s., Stream B, and also on one bulge for $U_0 = 90{\cdot}9$ f.p.s. in Stream A.

The results obtained are plotted in the form $(\Delta p/\frac{1}{2}\rho U_0^2)/(24h/\pi B)$ against $u_h h/\nu$ in Fig. 12, where Δp is the difference between the normal pressure on a bulge and that at the same station on the plate without a bulge, and u_h is the velocity at a distance h from the plate without a corrugation. The values of $u_h h/\nu$ were calculated from the relations given in Appendix (*b*).

The values of $(\Delta p/\frac{1}{2}\rho U_0^2)/(24h/\pi B)$ for the two speeds fall on the same curve for each value of x_1, where x_1 is the distance measured from the centre line of a bulge, except those for $x_1 = -0{\cdot}4B$. The results for this station can however be represented by the same curve if they are plotted in the form $\Delta p/\frac{1}{2}\rho U_0^2$ against h/δ, Fig. 13.

The values of $u_h h/\nu$ for the bulges when they just affect the position of transition lie within the range 1,000 to 3,000. Values of $(\Delta p/\frac{1}{2}\rho U_0^2)/(24h/\pi B)$ for these values of $u_h h/\nu$ are given in Table 6. They are in close agreement except those for $x_1 = 0{\cdot}5B$.

The values of $(\Delta p/\frac{1}{2}\rho U_0^2)$ are small, so that $\Delta p/\frac{1}{2}\rho U_0^2 = -2(\Delta u_1/U_0)$, where Δu_1 is the difference between the value of u_1 for the bulge and that for the plate without a bulge.

TABLE 6

Values of $\left(\frac{\Delta p}{\frac{1}{2}\rho U_0^2}\right)\Big/\left(\frac{24h}{\pi B}\right)$ *and* $-\left(\frac{\Delta u_1}{U_0}\right)\Big/\left(\frac{12h}{\pi B}\right)$

$\frac{x_1}{B}$	$\frac{u_h h}{\nu} = 1{,}000$	$\frac{u_h h}{\nu} = 3{,}000$
−0·700	+0·080	+0·080
−0·400	+0·330 (approx.)	+0·330
−0·175	−0·275	−0·280
+0·050	−0·690	−0·730
0·275	−0·280	−0·290
0·500	+0·060	−0·050
1·300	+0·020	+0·070

8.2. The theoretical distribution $(\Delta u_1/U_0)/(12h/\pi B)$ for a bulge (*see* Appendix (*c*)) is plotted in Fig. 14 (*a*) together with the measured distributions for

$$\frac{u_h h}{\nu} = 1{,}000 \text{ and } 3{,}000.$$

The measured distributions resemble the theoretical distribution, but there is a progressive departure in shape for the region near the after part of the bulge. In particular, the measured maximum value of $(\Delta u_1/U_0)/(12h/\pi B)$ is 0·74 the theoretical value.

Fig. 14 (*b*) gives the measured distributions of u_1/U_0 for the bulges. $h = 0{\cdot}070$ and 0·0555 in., in Stream A, and the bulges $h = 0{\cdot}062$ and 0·0525 in., in Stream B. The position of transition on the plate with a bulge moves forward with an increase in U_0 above the values for which the distributions were measured, but the distribution of u_1/U_0 remains the same, except for a small change near the after part of the bulge. Fig. 14 (*b*) shows that the value of u_1/U_0 falls with a near approach to a bulge, rises on the front part, and then falls on the after part. The numerical values of these gradients are large compared with that for the plate without a bulge.

8.3. Measured distributions of $(\Delta u_1/U_0)/(12h/\pi B)$ for hollows, when they begin to affect the transition position, are compared with the theoretical distribution in Fig. 15 (*b*). The resemblance between the measured and theoretical distributions is not so close at the front and closer behind than for a bulge (*cf.* Figs. 14 (*a*) and 15 (*b*)). The maximum value of $(\Delta u_1/U_0)/(12h/\pi B)$ is about 60 per cent. of the theoretical maximum. Fig. 15 (*c*) gives the measured distributions of u_1/U_0 for the hollows $h = 0{\cdot}067$ and 0·057 in. in Stream A. As for a bulge, the numerical values of the gradients of u_1/U_0 are large compared with that for the plate without a hollow.

8.4. It is seen in Fig. 14 (*b*) that there is a steep fall of u_1/U_0 in the region, $1{\cdot}48 < x < 1{\cdot}51$, near the front of a bulge. An average value for du_1/dx in this region is $-0{\cdot}36U_0$. Values of $(\vartheta/x)\ (U_0x/\nu)^{1/2}$, where ϑ is the momentum thickness, in this region for the plate without a bulge are 0·59 (Stream A) and 0·64 (Stream B). The negative gradient in u_1 near the front of the bulge causes a rapid increase in ϑ so that the value of $(\vartheta/x)\ (U_0x/\nu)^{1/2}$ there is greater than the value 0·59 for the plate without a bulge (Stream A). According to Howarth[4], separation of a laminar boundary layer from a surface occurs when $(\vartheta^2/\nu)\ (du_1/dx) = -0{\cdot}084$. For $(\vartheta/x)\ (U_0x/\nu)^{1/2} = 0{\cdot}59$ and $du_1/dx = -0{\cdot}36\ U_0$, $(\vartheta^2/\nu)\ (du_1/dx) = -0{\cdot}19$, so that the laminar boundary layer separates from the surface at the front of the bulge. The separated layer may rejoin the part of the bulge over which u_1/U_0 rises steeply (*see* Fig. 14 (*b*)), but whether this is so or not, it is to be expected that the layer is separated from the surface at the back of the bulge, where $du_1/dx = -0{\cdot}31U_0$ approx.

The value of $(\vartheta^2/\nu)\ (du_1/dx)$ for a smooth hollow is also less than the theoretical value for separation. It appears, therefore, that the flow conditions at a bulge or hollow when it affects

transition position beyond are associated with a separation of the laminar boundary layer from its surface.

8.5. Finally, it must be emphasised that the relations 1 and 2 for the minimum height, h, are empirical, and whilst they express reasonably adequately the results of both wind-tunnel and flight experiments, the extent to which extrapolation is permissible is not known. For example, for assigned values of X, u_{1c}, ν and B both relations show that h becomes very small when L is very large. The numerical value of a negative gradient of u_1 due to a bulge becomes smaller as h becomes smaller, so that the value of $(\vartheta^2/\nu)\,(du_1/dx)$ can then become greater than the theoretical value $-0{\cdot}084$ for laminar separation. Also, for assigned values of X, ν, B and L the value of $(\vartheta^2/\nu)\,(du_1/dx)$ can be greater than $-0{\cdot}084$, provided u_{1c} is sufficiently large and compressibility effects do not matter. The character of the flow near a corrugation may differ therefore from that described above when the values of L and u_{1c} are appreciably greater than the wind-tunnel values. Moreover, the effect of a corrugation on transition depends not only on the disturbance created near the bulge but also on the stability of flow in the boundary layer beyond. The problem is a difficult one and it is not to be expected that the simple relations given in the paper take into consideration all the conditions of flow involved.

APPENDIX

(*a*) *Ridge Shape.*—The theoretical shape of a ridge (and hollow) is that taken by a long strip, 4 in. wide, rigidly clamped at the longer edges and loaded uniformly along the centre line. The shape ordinates y are given by

$$y_1 = h\left[1 - 12\left(\frac{x_1}{B}\right)^2 - 16\left(\frac{x_1}{B}\right)^3\right] \text{ for } -\frac{B}{2} < x_1 < 0\,,$$

and

$$y_1 = h\left[1 - 12\left(\frac{x_1}{B}\right)^2 + 16\left(\frac{x_1}{B}\right)^3\right] \text{ for } 0 < x_1 < \frac{B}{2}\,,$$

where the origin is taken at the centre of the ridge width, and the positive direction of x_1 is in the direction of flow.

(*b*) *Plate Flow.*—Table 7 gives values of $(p - p_0)/\frac{1}{2}\rho U_0^2$ measured for the plate without a corrugation in Streams A and B, together with values of u_1/U_0 calculated from the relation

$$\frac{u_1}{U_0} = \left[1 - \frac{(p - p_0)}{\frac{1}{2}\rho U_0^2}\right]^{1/2}.$$

TABLE 7

x ft.	Stream A		Stream B	
	$\frac{(p - p_0)}{\frac{1}{2}\rho U_0^2}$	$\frac{u_1}{U_0}$	$\frac{(p - p_0)}{\frac{1}{2}\rho U_0^2}$	$\frac{u_1}{U_0}$
0·042	0·458	0·736	0·143	0·925
0·083	0·386	0·782	0·190	0·900
0·250	0·220	0·882	0·120	0·937
0·417	0·138	0·927	0·066	0·967
0·833	0·074	0·963	0·042	0·979
1·250	+0·031	0·985	+0·018	0·991
2·083	−0·024	1·012	−0·012	1·006
2·917	−0·059	1·029	−0·028	1·014
3·750	−0·089	1·043	−0·039	1·020
4·583	−0·119	1·057	−0·053	1·026

The solution of the laminar boundary-layer equations for the distributions of u_1/U_0 in Table 7 gave the following results for the region $x/X = 0{\cdot}9$ to $1{\cdot}1$:—

$$\text{Stream A, } \frac{\vartheta}{x}\left(\frac{U_0 x}{\nu}\right)^{1/2} = 0{\cdot}59 \text{ and } \frac{\delta}{x}\left(\frac{U_0 x}{\nu}\right)^{1/2} = 5{\cdot}0 .$$

$$\text{Stream B, } \frac{\vartheta}{x}\left(\frac{U_0 x}{\nu}\right)^{1/2} = 0{\cdot}64 \text{ and } \frac{\delta}{x}\left(\frac{U_0 x}{\nu}\right)^{1/2} = 5{\cdot}5 .$$

The momentum thickness ϑ was determined from the relation

$$\vartheta^2 = \frac{0{\cdot}470\nu}{u_1^{6{\cdot}28}} \int_0^x u_1^{5{\cdot}28}\, dx ,$$

(*see* Appendix II of Ref. 5), and the thickness δ from the value of ϑ by the Kármán-Pohlhausen relation

$$\vartheta = \frac{\delta}{315}\left(37 - \frac{\Lambda}{3} - \frac{5\Lambda^2}{144}\right).$$

The velocity u in the boundary layer was determined from the Kármán-Pohlhausen relation

$$\frac{u}{u_1} = \left(\frac{12+\Lambda}{6}\right)\frac{y}{\delta} - \frac{\Lambda}{2}\left(\frac{y}{\delta}\right)^2 - \left(\frac{4-\Lambda}{2}\right)\left(\frac{y}{\delta}\right)^3 + \left(\frac{6-\Lambda}{6}\right)\left(\frac{y}{\delta}\right)^4 .$$

(*c*) *Theoretical Velocity Distribution.*—A close approximation to the velocity distribution for irrotational two-dimensional flow past a smooth bulge on an infinite flat plate in a stream of velocity U_0 is given, when h/B is small, by the relation

$$\frac{q}{U_0} = 1 + \frac{\Delta u_1}{U_0} = 1 - \frac{1}{\pi} P \int_{-\infty}^{\infty} \frac{y'(\xi)}{(\xi - x)}\, d\xi , \quad \ldots \quad \ldots \quad \ldots \quad \ldots \quad \ldots \quad (3)$$

where q is the surface velocity,

Δu_1 is the excess surface velocity at the position x,

$y(\xi)$ is the displacement of a point on the bulge from the x-axis, the origin of the x-axis being on the centre line of the bulge,

P denotes that the principal value of the integral is to be taken and the dash denotes a derivative.

This relation is given, in different notation, in Appendix II of Ref. 6 (*see also* Goldstein[7]).

The calculated shape of a bulge is given (*see* Appendix (*a*) above)

by $$y(\xi) = h\left[1 - 12\left(\frac{\xi}{B}\right)^2 - 16\left(\frac{\xi}{B}\right)^3\right] \text{ for } -\frac{B}{2} < \xi < 0$$

and $$y(\xi) = h\left[1 - 12\left(\frac{\xi}{B}\right)^2 + 16\left(\frac{\xi}{B}\right)^3\right] \text{ for } 0 < \xi < \frac{B}{2} .$$

Also $y(\xi) = 0$ for $-\infty < \xi < -(B/2)$ and $(B/2) < \xi < \infty$. The solution of the relation (3) gives

$$\frac{q}{U_0} = 1 + \frac{\Delta u_1}{U_0}$$

$$= 1 + \frac{12h}{\pi B}\left\{1 + \frac{2x}{B}\left(\log_e\left|1 - \frac{2x}{B}\right| - \log_e\left|1 + \frac{2x}{B}\right|\right) - \left(\frac{2x}{B}\right)^2\left(\log_e\left|\frac{B}{2x} + 1\right| + \log_e\left|\frac{B}{2x} - 1\right|\right)\right\}.$$

The numerical value of $\Delta u_1/U_0$ for a smooth hollow is the same as that for a smooth bulge but the sign is negative.

(*d*) *Surface Tube Technique.*—The pressure at the mouth of a tube was measured against the static pressure at a hole on the centre line of the plate at the same distance behind the leading edge (Fig. 3).

The reading r of a surface tube is $\frac{1}{2}\rho[h_e(du/dy)_0]^2$, where h_e is the effective distance from the surface to which the velocity measured by the tube is related and $(du/dy)_0$ is the velocity gradient at the surface. For laminar flow in the boundary layer and an assigned distribution of u_1/U_0. the values of (δ/x) $(u_1x/\nu)^{1/2}$ and Λ are constants for a given value of x.

Also, $$\left(\frac{du}{dy}\right)_o = \left(\frac{12 + \Lambda}{6}\right)\frac{u_1}{\delta},$$

according to the Kármán-Pohlhausen solution of the laminar boundary-layer equations, so that $(1/h_e)$ $(r/U_0^3)^{1/2}$, where U_0 is the datum stream velocity, is a constant. The readings taken for laminar flow in the boundary layer showed that $(r/U_0^3)^{1/2}$ was either constant or changed little with U_0. The effective distance h_e could therefore be taken to be a constant. Further, there was no need to calibrate a surface tube, for an increase in the value of $(1/K)$ $(r/U_0^3)^{1/2}$ from unity, where K is the value of $(r/U_0^3)^{1/2}$ obtained for laminar flow, then indicates a change from laminar flow. The value of U_0 for which the change occurs is that for transition at the position of the surface tube.

REFERENCES

No.	*Author*	*Title, etc.*
1	Fage, A. and Preston, J. H.	On Transition from Laminar to Turbulent Flow in the Boundary Layer. *Proc. Roy. Soc. A.*, Vol. 178, 1941, pp. 201–227.
2	Squire, H. B. and Johnstone, W. S.	Third Interim Note on Flight Tests of Low-drag Sections at the R.A.E. R.A.E. Departmental Note—Full Scale No. 103. A.R.C. 5416. September, 1941. (Unpublished.)
3	The Staffs of the S.M.E. and Aero Departments, R.A.E.	The Design of Smooth Wings. R.A.E. Report S.M.E. 3236. A.R.C. 6334. November, 1942. (Unpublished.)
4	Howarth, L.	On the Solution of Laminar Boundary-layer Equations. *Proc. Roy. Soc.* A., Vol. 164, 1938, pp. 547–579.
5	Young, A. D. and Winterbottom, N. E.	Note on the Effect of Compressibility on the Profile Drag of Aerofoils in the absence of Shock Waves. R.A.E. Report B.A. 1595. A.R.C. 4667 (Appendix II). July, 1940. (To be published.)
6	Pringle, G. E., Squire, H. B. and Lush, K. T.	Flight Tests of Wing Sections designed for Low Drag. R.A.E. Report Aero 1723. A.R.C. 5677 (Appendix II). January, 1942. (Unpublished.)
7	Goldstein, S.	A Theory of Aerofoils of Small Thickness, Part I. Velocity Distributions for Symmetrical Aerofoils. A.R.C. 5804. May, 1942. (To be published.)

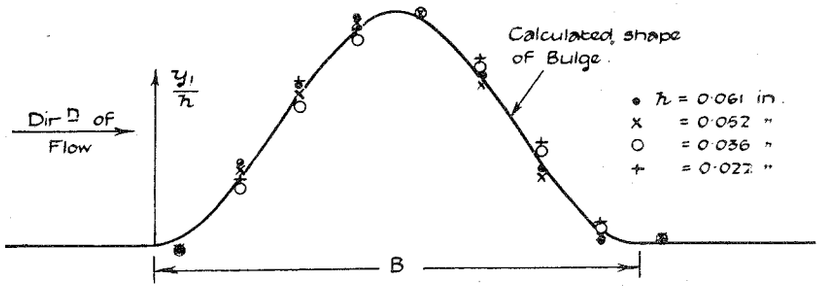

FIG. 2.

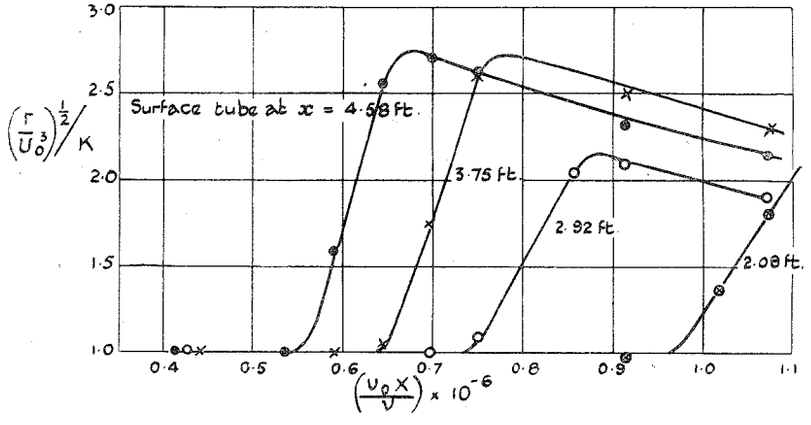

Smooth bulge. $h = 0{\cdot}062$ in. $B = 4$ in. $A_X = 0{\cdot}9$.

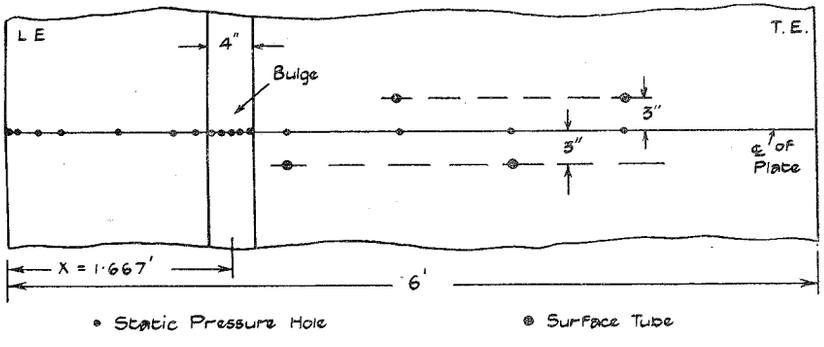

FIG. 3.

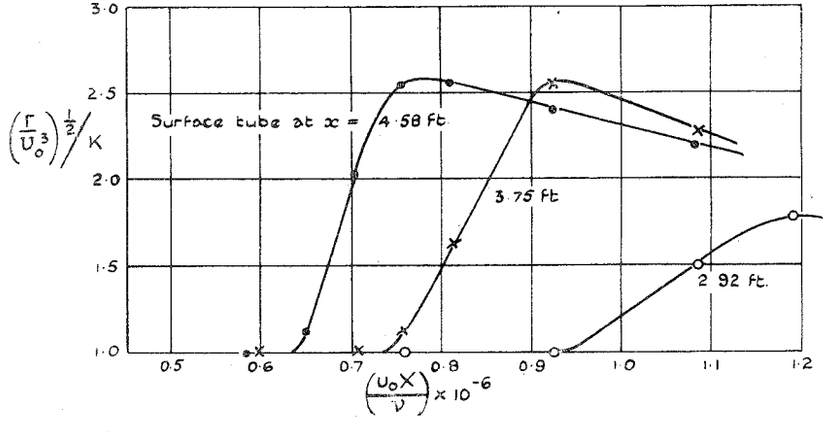

Flat ridge. $h = 0{\cdot}0245$ in. $B = 0{\cdot}9$ in. $A_X = 0{\cdot}9$.

FIG. 5.

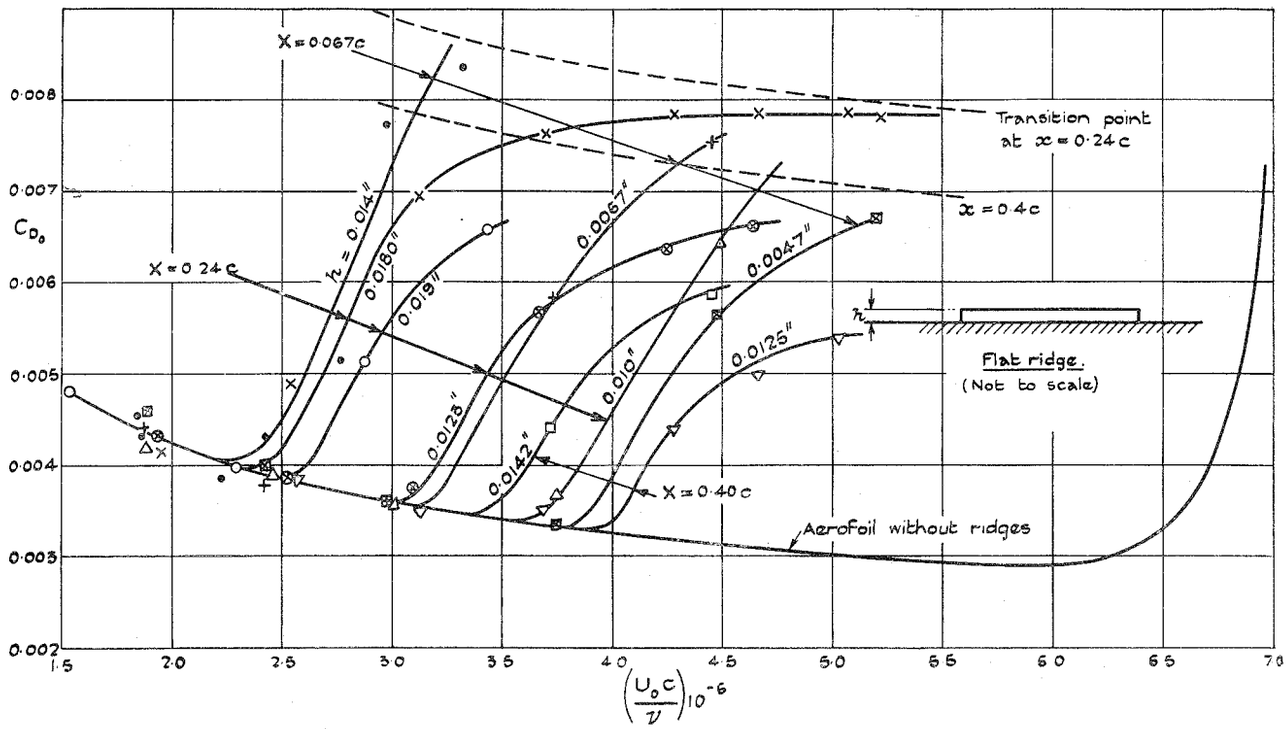
X = 0·067c
Transition point at x = 0·24c
x = 0·4c
X = 0·24c
h = 0·014"
0·0180"
0·019"
0·0067"
0·0047"
0·010"
0·0125"
0·0128"
0·0142"
X = 0·40c
Aerofoil without ridges
h
Flat ridge.
(Not to scale)
C_{D_0}
0·008
0·007
0·006
0·005
0·004
0·003
0·002
1·5
2·0
2·5
3·0
3·5
4·0
4·5
5·0
5·5
6·0
6·5
7·0
$\left(\frac{U_0 c}{\nu}\right) 10^{-6}$

FIG. 6.

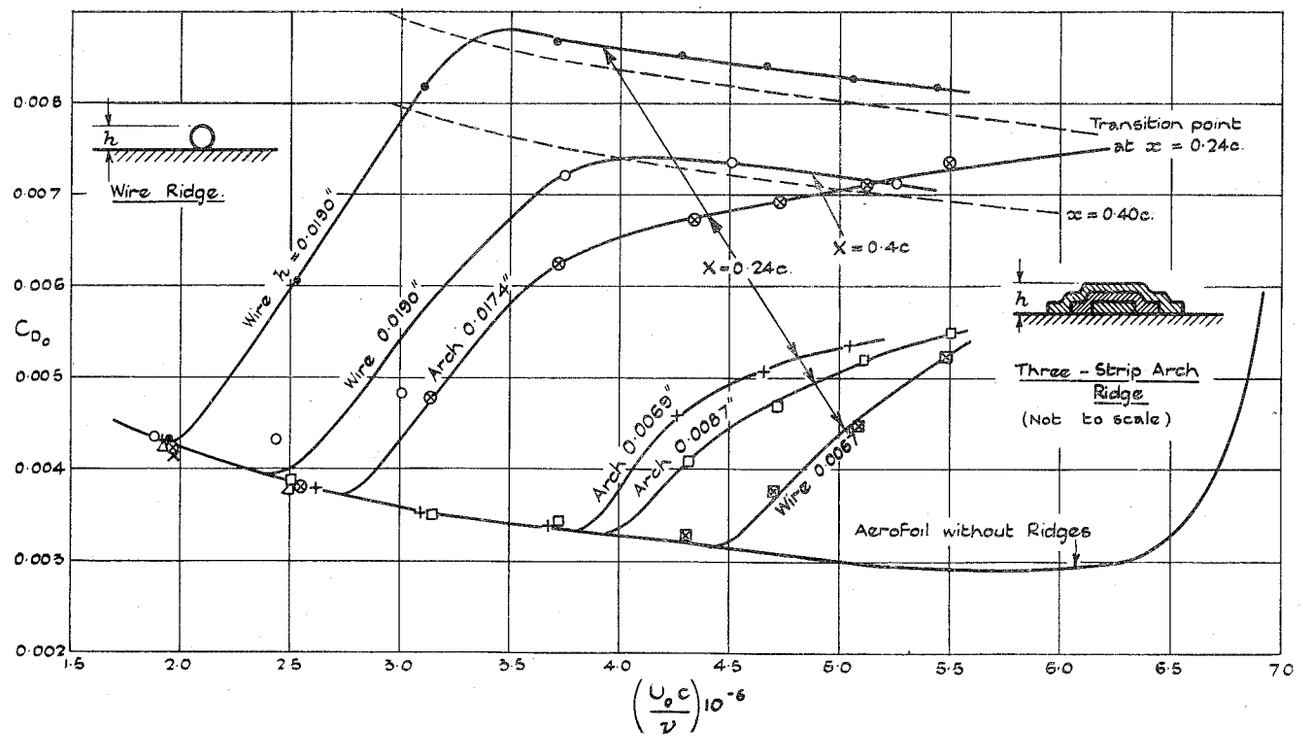
h
Wire Ridge.
Wire h = 0·0190"
Wire 0·0190"
Arch 0·0174"
Transition point at x = 0·24c.
x = 0·40c.
X = 0·4c
X = 0·24c.
Arch 0·0059"
Arch 0·0087"
Wire 0·0067"
Aerofoil without Ridges
h
Three - Strip Arch Ridge
(Not to scale)
C_{D_0}
0·008
0·007
0·006
0·005
0·004
0·003
0·002
1·5
2·0
2·5
3·0
3·5
4·0
4·5
5·0
5·5
6·0
6·5
7·0
$\left(\frac{U_0 c}{\nu}\right) 10^{-6}$

FIG. 7.

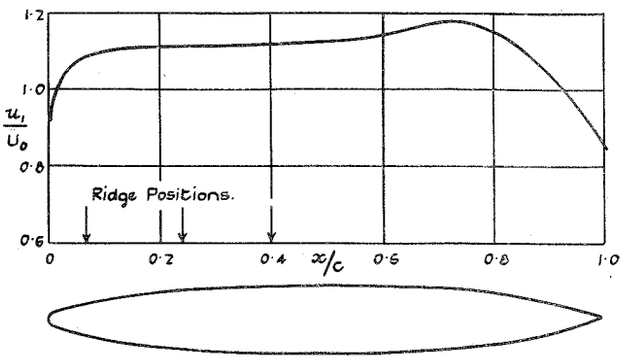

FIG. 8.—Aerofoil EQH 1260. 0 deg. Incidence.

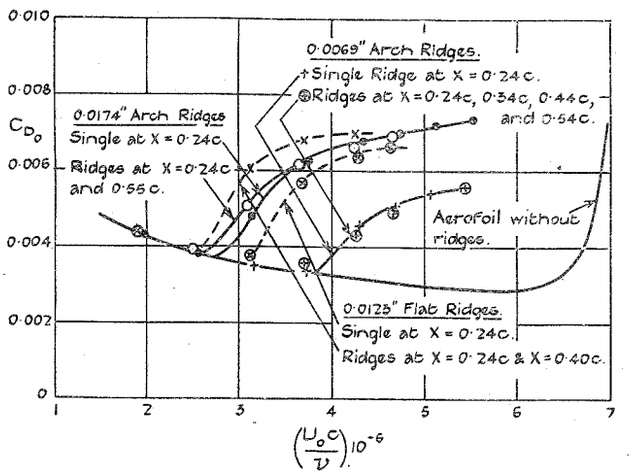

FIG. 9.

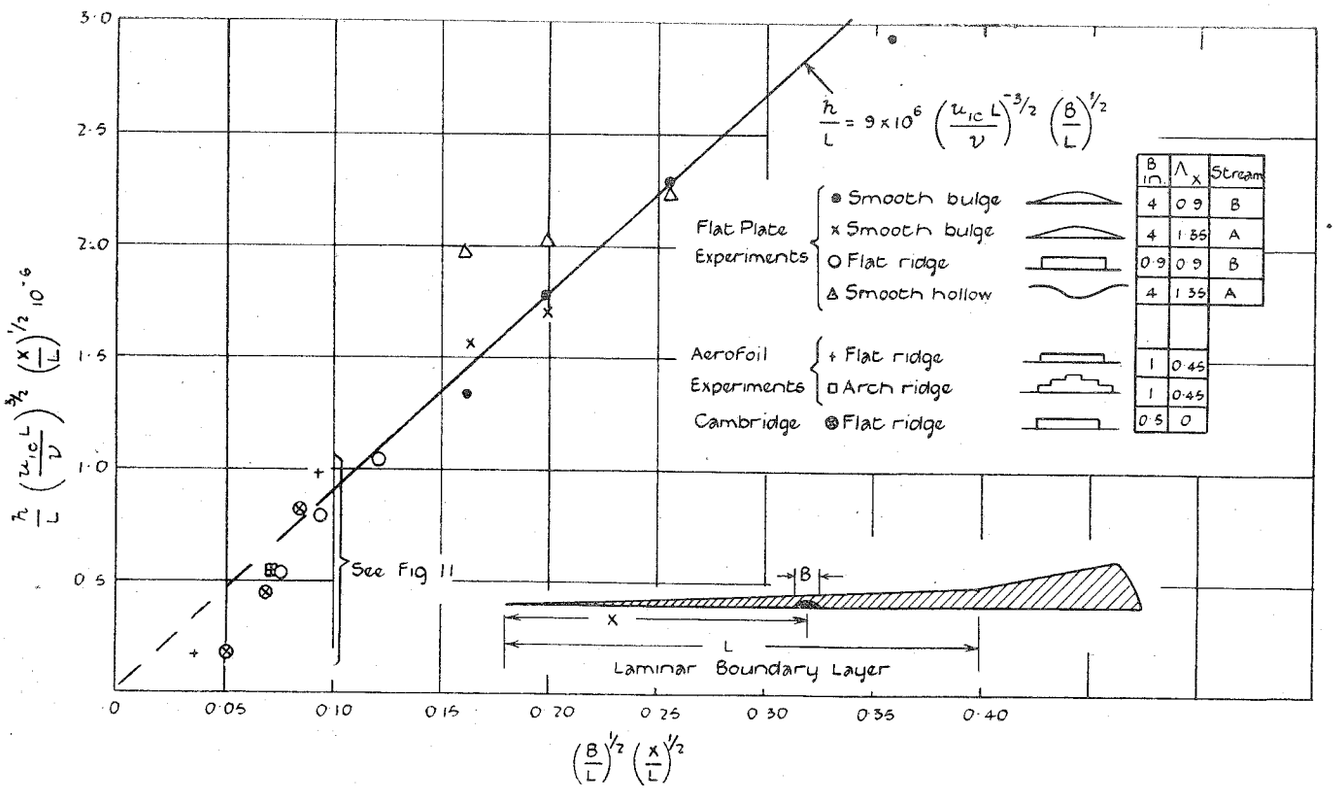

FIG. 10.

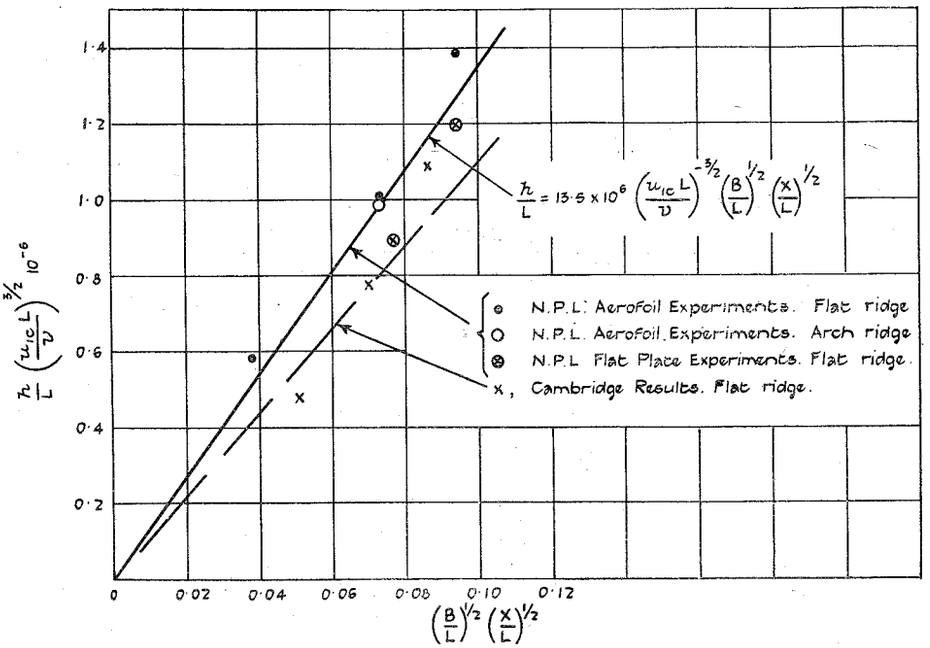
$\frac{h}{L} = 13{\cdot}5 \times 10^{6} \left(\frac{u_{1c}L}{\nu}\right)^{-3/2} \left(\frac{B}{L}\right)^{1/2} \left(\frac{X}{L}\right)^{1/2}$
N.P.L. Aerofoil Experiments. Flat ridge
N.P.L. Aerofoil Experiments. Arch ridge
N.P.L Flat Plate Experiments. Flat ridge.
x, Cambridge Results. Flat ridge.
$\frac{h}{L}\left(\frac{u_{1c}L}{\nu}\right)^{3/2} 10^{-6}$
$\left(\frac{B}{L}\right)^{1/2}\left(\frac{X}{L}\right)^{1/2}$

FIG. 11.

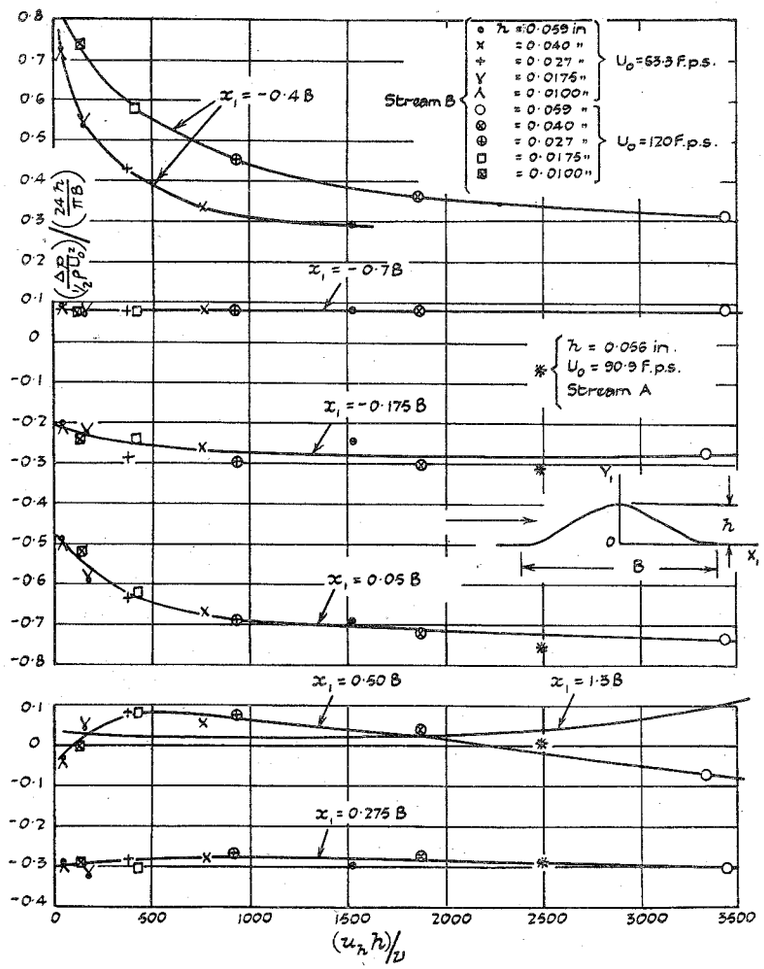
Stream B
h = 0·059 in
= 0·040 "
= 0·027 "
= 0·0175"
= 0·0100"
U_0 = 63·3 F.p.s.
U_0 = 120 F.p.s.
$x_1 = -0{\cdot}4B$
$x_1 = -0{\cdot}7B$
$x_1 = -0{\cdot}175B$
$x_1 = 0{\cdot}05B$
$x_1 = 0{\cdot}50B$
$x_1 = 1{\cdot}3B$
$x_1 = 0{\cdot}275B$
h = 0·056 in.
U_0 = 90·9 F.p.s.
Stream A
$\left(\frac{\Delta p}{\frac{1}{2}\rho U_0^2}\right)\left(\frac{24h^2}{\pi B}\right)$
$(u_x h)/\nu$

FIG. 12.

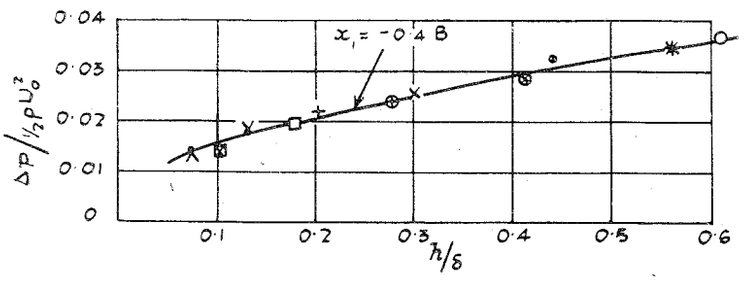

FIG. 13.

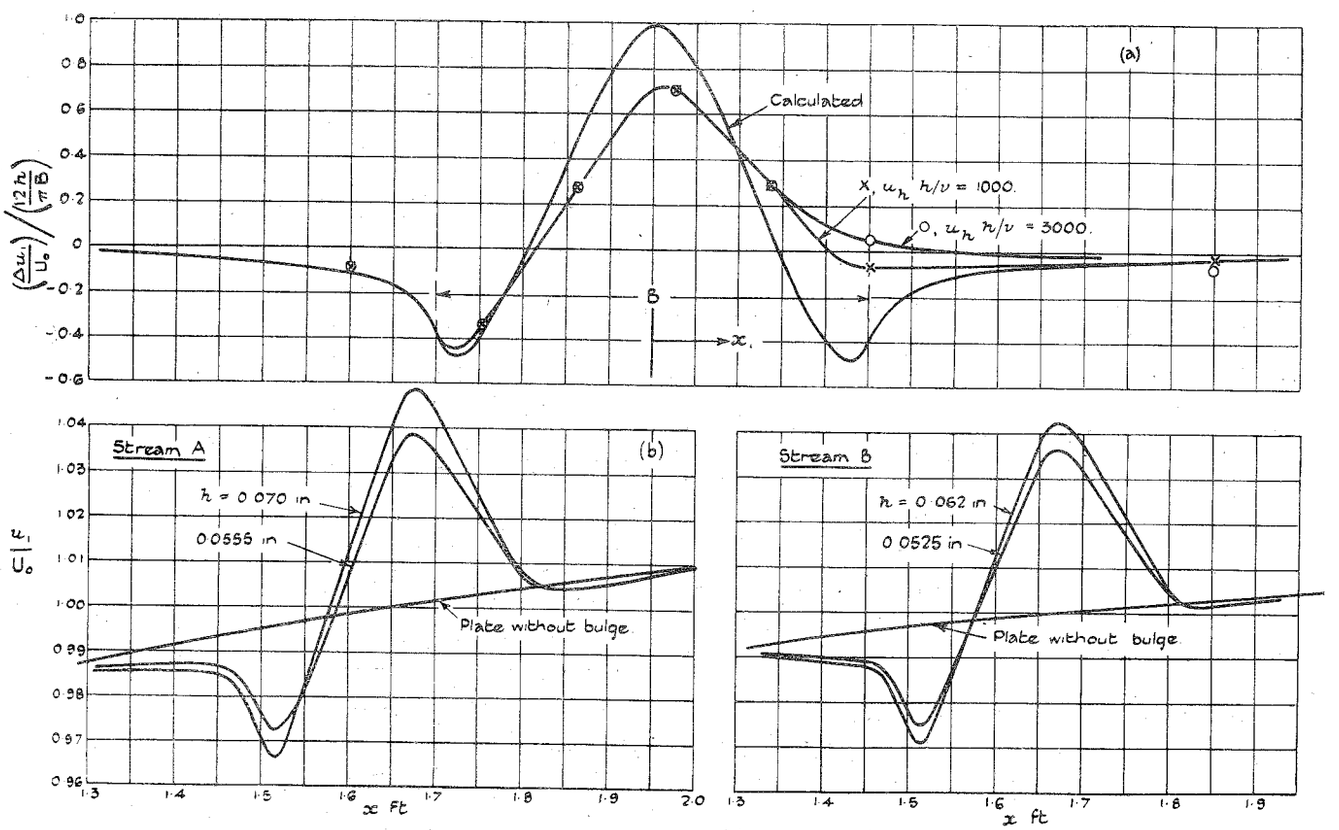

FIG. 14.—Smooth Bulges.

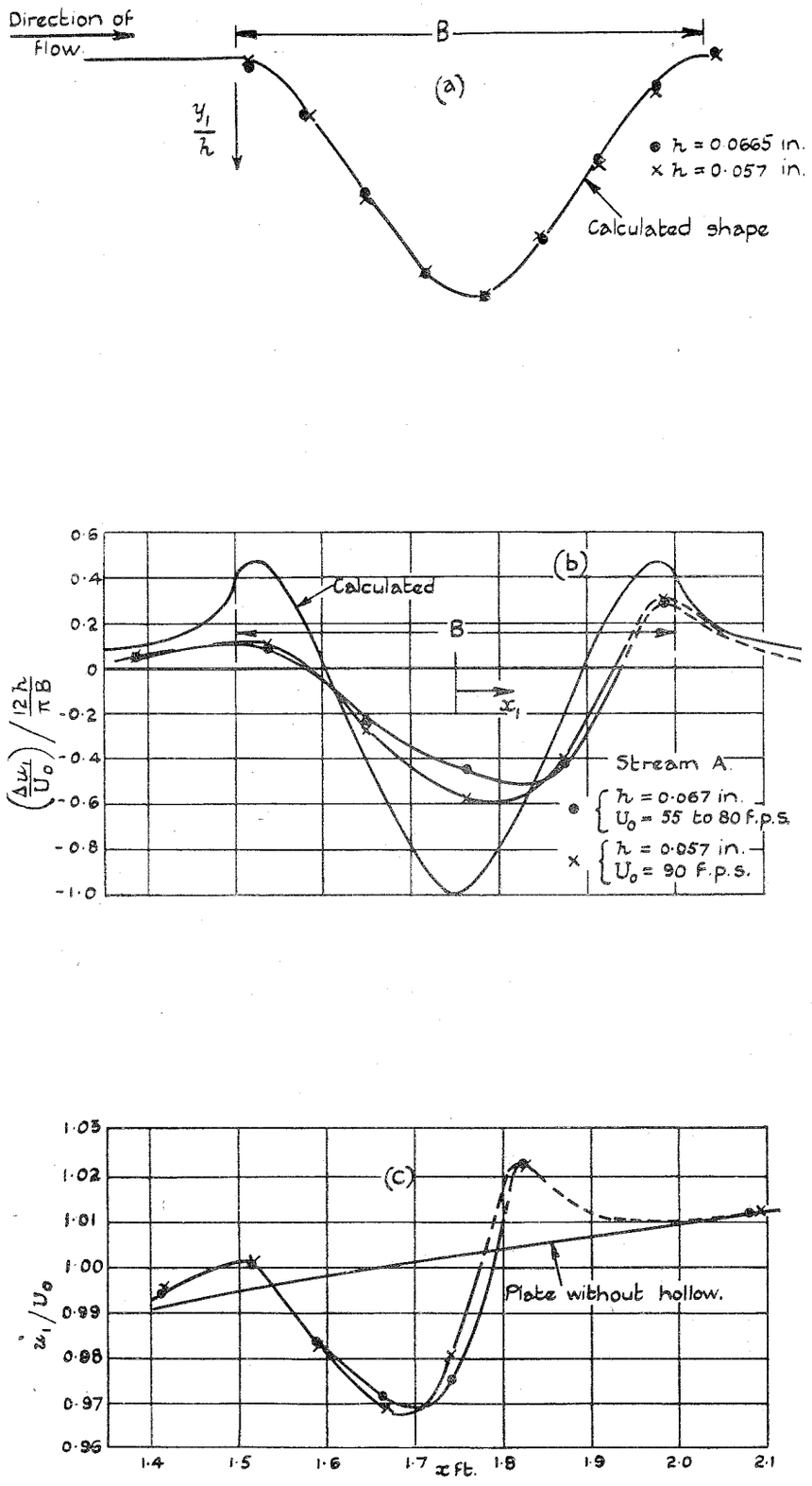

FIG. 15.—Smooth Hollows.

(77253) Wt. 10/7116 6/47 Hw. G.377/1